

NATIONAL ADVISORY COMMITTEE FOR AERONAUTICS

TECHNICAL NOTE 3504

EFFECT OF TRAILING-EDGE THICKNESS ON LIFT
AT SUPERSONIC VELOCITIES

By Dean R. Chapman and Robert H. Kester

Ames Aeronautical Laboratory
Moffett Field, Calif.



Washington

June 1955

AFM26
TECHNICAL LIBRARY
JUL 20 1955



0066616

TECHNICAL NOTE 3504

EFFECT OF TRAILING-EDGE THICKNESS ON LIFT
AT SUPERSONIC VELOCITIES¹

By Dean R. Chapman and Robert H. Kester

SUMMARY

Measurements of lift were made on various rectangular-plan-form wings differing in trailing-edge thickness, profile shape, maximum thickness ratio, and aspect ratio. The experiments were conducted at Mach numbers between 1.5 and 3.1, at Reynolds numbers between 0.55 and 2.2 million, and on wings with and without boundary-layer trips. The measurements are compared to theoretical calculations based on both second-order and shock-expansion theory. Calculated results using shock-expansion theory are presented for Mach numbers between 1.5 and 10.

In all cases the experimental values of lift-curve slope for wings having a blunt trailing edge were higher than those for wings of equal thickness ratio having a sharp trailing edge, with the difference in most cases varying from a few percent to about 15 percent, depending primarily on trailing-edge thickness. The agreement between theoretical calculations and experiment was reasonably good. The calculations for 5-percent-thick airfoils at 5° angle of attack in the Mach number range between 7 and infinity indicate between about 15- and 25-percent-higher lift for full-blunt airfoils than for sharp-trailing-edge airfoils.

INTRODUCTION

The use of airfoils with appreciable trailing-edge thickness has received little attention prior to the last few years presumably because of the high drag associated with a blunt trailing edge at low speeds. Recently the aerodynamic characteristics of blunt-trailing-edge airfoils at high velocities have been investigated considerably both through experiments and theoretical analyses. Such investigations have been conducted partly because of the evident structural advantages of employing a moderately thick trailing edge, and also partly because of several aerodynamic advantages that exist under some conditions. Some of these aerodynamic advantages observed from experiments are: an improvement in

¹Supersedes recently declassified NACA RM A52D17 by Dean R. Chapman and Robert H. Kester, 1952.

certain lift and control characteristics at transonic velocities, a reduction in profile drag at moderate and high supersonic velocities, and an increase in lift-curve slope at supersonic velocities. The present investigation is concerned solely with the lift characteristics of blunt-trailing-edge wings in supersonic flow.

The first indication of possible increases in lift-curve slope through the use of a thick trailing edge at supersonic velocities was given by the calculations and experiments of Busemann and Walchner (reference 1). These calculations have been elaborated in reference 2, and partially verified by the experiments of that investigation which showed in one case a 17-percent-higher lift-curve slope for a 10-percent-thick blunt-trailing-edge wing than for a sharp-trailing-edge wing of equal thickness.

The purposes of this report are (1) to determine experimentally the extent to which theoretical calculations predict the increase in lift-curve slope attainable by using a thick trailing edge at supersonic Mach numbers up to 3, and (2) to present results based on shock-expansion calculations of the theoretical increase in lift-curve slope attainable at Mach numbers up to 10.

NOTATION

A	aspect ratio
c	airfoil chord
C_L	lift coefficient $\left(\frac{L}{q_\infty S}\right)$
ΔC_L	lift coefficient of blunt-trailing-edge airfoil minus lift coefficient of sharp-trailing-edge airfoil of equal maximum thickness ratio
L	lift force
h	trailing-edge thickness
M	Mach number
p	static pressure
P_b	base pressure coefficient $\left(\frac{p_b - p_\infty}{q_\infty}\right)$
q	dynamic pressure
Re	Reynolds number based on wing chord and free-stream condition

t	maximum airfoil thickness
S	wing plan-form area
s	chordwise distance from leading edge to first position of maximum thickness
x	chordwise distance from leading edge
y	ordinate of airfoil surface measured from chord line
$\Delta \left(\frac{dC_L}{d\alpha} \right)$	lift-curve slope of blunt-trailing-edge airfoil minus lift-curve slope of sharp-trailing-edge airfoil; both slopes evaluated at $\alpha = 0^\circ$
α	angle of attack
β	boattail angle (one-half the total included trailing-edge angle)
ν	ratio of specific heats (1.40 for air)
θ, λ	angles defining airfoil shape (See fig. 2.)

Subscripts

o	sharp-trailing-edge airfoil
∞	free stream
b	base

APPARATUS AND TEST PROCEDURE

Wind Tunnel and Balance

Experiments were conducted in the Ames 1- by 3-foot supersonic wind tunnels No. 1 and No. 2. The No. 1 tunnel is of the closed-circuit continuous-operation type, and the No. 2 tunnel is of the blowdown type. Both tunnels are equipped with flexible-plate nozzles for varying the test Mach number. Reynolds number variation is accomplished by changing the absolute pressure level. In order to minimize effects of humidity on the supersonic flow, the specific humidity throughout the investigation was maintained at less than 0.0003 pound water vapor per pound of dry air.

Aerodynamic forces and moments acting on each model were measured by means of a three-component electrical-strain-gage balance shielded from the oncoming flow in the manner indicated by the photographs of figure 1. Strain-gage temperatures, as measured by thermocouples connected to a recording potentiometer, were used to correct each gage reading for the small temperature effect.

Models and Supports

Wings employed for this investigation were made of steel with ground and polished surfaces. To simplify their construction, they were all of rectangular plan form with uncambered airfoil sections. Three of the wings on which force measurements were taken are shown in the photographs of figure 1. The various wings investigated, details of which are given in figure 2, were divided into three groups according to airfoil shape forward of the trailing edge. Wings of the first group were constructed with straight sides and differed primarily in maximum thickness ratio t/c and trailing-edge thickness ratio h/t . (See fig. 2(a).) This same group of wings, termed the "thickness group," was employed in the base-pressure investigation of reference 3, and most of the present data for these wings were obtained simultaneously with the base pressure data of that reference. The second group of wings, profiles of which are shown in figure 2(b), also were constructed with straight sides. Wings of this group, termed the "boattail group," differed primarily in boattail angle (one-half the trailing-edge angle), and were employed in the investigation of reference 3. The third group of wings, profiles of which are given in figure 2(c), were constructed with circular-arc airfoil sections. Wings of this group, termed the "circular-arc group," were employed in the investigation of reference 2.

All wings tested were supported from the rear as shown by the photographs of figure 1. Asymmetric stings (fig. 1(c)) were permanently attached to the wings with circular-arc contours at an initial angle of incidence of 4.5° , which, together with the $\pm 5.5^\circ$ angle range of the balance, provided a range of nominal angles of attack from -1° to $+10^\circ$. The nominal angle-of-attack range for the wings with straight sides was $\pm 5.5^\circ$, as these wings were tested with the symmetrical body supports and sting supports (figs. 1(a) and 1(b)).

Test Methods and Reduction of Data

Over most of the range of Reynolds numbers investigated in the present tests, laminar flow was expected over the entire surface of a smooth wing. This expectation was verified by the China-clay technique

as shown in reference 3. Hence, in order to simulate the case of a turbulent boundary layer over the rear portion of the chord, it was necessary to add a boundary-layer trip to the wing surfaces. Several different types of trip were used for this purpose. On the wings with circular-arc airfoils a cotton thread of approximately 0.006-inch diameter was cemented spanwise to both the upper and lower surfaces at approximately the 20-percent-chord position. On the wings with straight sides, which had a longer chord, it was found sufficient and more convenient to use either a 0.005-inch wire or a band of lampblack. Figure 1(a) shows a wing of the thickness group with the wire trip attached. The existence of turbulent boundary layers with the various types of roughness was confirmed by the afore-mentioned China-clay technique. (See reference 3.)

Angles of attack were determined by adding to the nominal angle of attack a deflection allowance as calculated from the measured forces and moments and the predetermined elastic constants. Pressure data required for the evaluation of Reynolds number, local dynamic pressure, and the balance-chamber-pressure correction were obtained by means of a multiple-tube mercury manometer. Mach number was determined from tunnel surveys made before the wings were installed.

Force measurements were taken in 1° increments from small negative angles of attack to the highest positive angles provided. A typical set of lift curves so obtained is shown in figure 3. These particular data are for 10-percent-thick airfoils of the circular-arc group of wings with smooth surfaces. It may be noted that extrapolation of the lift curves would indicate intersection at a point below and to the left of the origin. This is caused by the tunnel stream angle and by the aerodynamic tare forces acting on the asymmetric stings. A numerical value for the slope of each experimentally determined lift curve was computed by the method of least squares employing only the linear portion of the curve. All measured data have been converted to the form of a fractional increase in lift-curve slope relative to the lift-curve slope of the basic sharp-trailing-edge wing of each family. Thus

$$\frac{\Delta \left(\frac{dC_L}{d\alpha} \right)}{\left(\frac{dC_L}{d\alpha} \right)_0} \equiv \frac{\frac{dC_L}{d\alpha} - \left(\frac{dC_L}{d\alpha} \right)_0}{\left(\frac{dC_L}{d\alpha} \right)_0} \quad (1)$$

where the subscript 0 designates the basic sharp-trailing-edge wing having the same thickness ratio as the blunt-trailing-edge wing and tested with the same support, in the same stream, and at the same position in the test section. The sting tare forces and the differences in lift curves were not large. It was unnecessary to apply corrections for tare forces, or for the small variations in stream angle existing in the

test section, inasmuch as all subsequent data are presented in the incremental form indicated by the above equation. Absolute values of $\frac{dC_L}{d\alpha}$ and $\left(\frac{dC_L}{d\alpha}\right)_0$ are not presented, as such quantities are affected appreciably by support tares and stream-angle variations.

THEORETICAL CALCULATIONS

As a basis of comparison for experimental results at moderate supersonic Mach numbers (say, between 1.5 and 3), calculations using either second-order airfoil theory or shock-expansion theory can be employed. If second-order theory is employed, the fractional increase in lift-curve slope for any profile is (see references 1 and 2)

$$\frac{\Delta\left(\frac{dC_L}{d\alpha}\right)}{\left(\frac{dC_L}{d\alpha}\right)_0} = \frac{h}{c} \left[\frac{(\gamma + 1)M_\infty^4 - 4(M_\infty^2 - 1)}{4(M_\infty^2 - 1)^{3/2}} \right] \quad (2)$$

In deriving this equation, the lift force contributed by the pressure acting on the base has been neglected. If the base force were considered, an

additional term $P_b h \sqrt{M_\infty^2 - 1} / 4c$ would appear on the right side of equation (2). For full blunt airfoils of 10-percent-thickness ratio, for example, the maximum relative contribution of base pressure to the total lift force amounts to about 1 percent. In this case, 1 percent of

the total lift corresponds to about 7 percent of $\Delta\left(\frac{dC_L}{d\alpha}\right) / \left(\frac{dC_L}{d\alpha}\right)_0$,

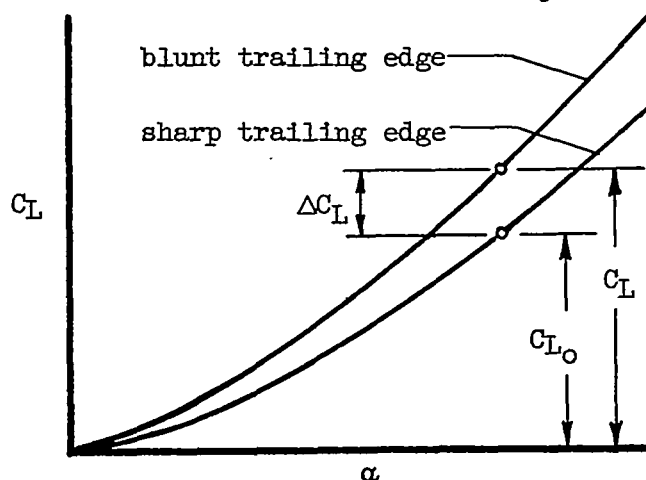
which is somewhat less than the experimental accuracy. Inasmuch as the contribution of base pressure to lift is less for thinner airfoils, and also approaches zero at high supersonic Mach numbers, it is neglected throughout this report.

In making theoretical lift calculations for Mach numbers above about 3 where second-order theory no longer provides an accurate approximation, shock-expansion theory can be employed although it leads to two complications. First, the lift-curve slope depends not only on M_∞ and h/c , but also on the entire shape of the profile forward of the trailing edge;

hence no simple analytical formula for $\Delta\left(\frac{dC_L}{d\alpha}\right) / \left(\frac{dC_L}{d\alpha}\right)_0$ can be

exhibited, and numerical computations have to be made for each airfoil at each Mach number. Second, the lift curves are nonlinear, thereby introducing additional dependence on α . As would be expected, however,

this nonlinearity introduced by shock-expansion theory is negligible at moderate supersonic Mach numbers, but can be important at hypersonic Mach numbers. Consequently, the quantity $\Delta C_L / C_{L_0}$ is used later as a



basis of comparison for hypersonic Mach numbers rather than

$\Delta \left(\frac{dC_L}{d\alpha} \right) / \left(\frac{dC_L}{d\alpha} \right)_0$. The two quantities coincide, of course, if the lift curves are linear.

RESULTS AND DISCUSSION

Since the theoretical calculations for airfoils might not apply with adequate accuracy to the plan-form regions within the tip Mach cones, some measurements of lift-curve slope were obtained on wings with constant chord and varying span. The results are shown in figure 4 plotted as a function of the fraction of wing area blanketed by the tip Mach cones. For both the thickness group and circular-arc group of airfoils, the effect of aspect ratio (slope of various curves in fig. 4) on the fractional increase in lift-curve slope is appreciable, but is much smaller than the maximum observed effect of airfoil profile shape (maximum spacing between curves in fig. 4). In view of this fact, and the fact that the area blanketed by tip Mach cones was relatively small for many of the cases investigated, it is reasonable to compare calculated results based on two-dimensional-airfoil theory with experimental results obtained on the finite-span wings.

Comparison of Experimental Results With Theory at
Moderate Supersonic Mach Numbers

In figure 5 the various experimental values of $\Delta \left(\frac{dC_L}{d\alpha} \right) / \left(\frac{dC_L}{d\alpha} \right)_0$ are compared with the values calculated from both second-order and shock-expansion theory.² It is seen that in all cases $\Delta \left(\frac{dC_L}{d\alpha} \right) / \left(\frac{dC_L}{d\alpha} \right)_0$ is positive, indicating that the blunt-trailing-edge wings had higher lift-curve slopes than the corresponding sharp-trailing-edge wings. The results in figures 5(a), 5(b), and 5(c), which were obtained with the body support at Mach numbers of 1.5, 1.9, and 3.1, respectively, indicate that the fractional increase in lift-curve slope is predicted reasonably well by shock-expansion theory. The values of $\Delta \left(\frac{dC_L}{d\alpha} \right) / \left(\frac{dC_L}{d\alpha} \right)_0$ increase somewhat as the Mach number increases. The results in figure 5(d), which were obtained with the sting support at a Mach number of 2.0, also agree approximately with the theoretical calculations, although in this figure the shock-expansion theory appears no better than second-order theory. This inconsistency is not necessarily due to the different supports, since the difference between the data of figures 5(b) and 5(d) is of the same order of magnitude as the estimated experimental uncertainty.

In figure 5(e) experimental values of $\Delta \left(\frac{dC_L}{d\alpha} \right) / \left(\frac{dC_L}{d\alpha} \right)_0$ are presented for wings of the boattail group, where $\left(\frac{dC_L}{d\alpha} \right)_0$ again corresponds to the doubly symmetric double wedge of the same thickness. Although the boattail angle of these wings varies from 0° to 20° , no systematic variation of $\Delta \left(\frac{dC_L}{d\alpha} \right) / \left(\frac{dC_L}{d\alpha} \right)_0$ with boattail angle was observed; consequently, boattail angles are not designated in figure 5(e). Again the results appear to be in reasonable agreement with second-order theory. Calculations based on shock-expansion theory were not made for this group of wings.

²The calculations employing shock-expansion theory actually represent $\Delta C_L / C_{L_0}$ at $\alpha = 5^\circ$ rather than $\Delta(dC_L/d\alpha)/(dC_L/d\alpha)_0$ at $\alpha = 0^\circ$. The difference between these two quantities, however, is negligible for the Mach number range of the experiments inasmuch as the lift curves in this range are practically linear.

It is to be noted that the tagged symbols in figure 5, which represent wings with a boundary-layer trip, do not differ significantly from the other data shown in figures 5(a) to 5(e). This indicates that the transition from laminar to turbulent flow on wings of the thickness and

boattail groups does not materially affect $\Delta \left(\frac{dC_L}{d\alpha} \right) / \left(\frac{dC_L}{d\alpha} \right)_0$. Such is

not the case, however, for wings of the circular-arc group at $M_\infty = 1.5$, as is illustrated in figure 5(f). The fractional increase in lift-curve slope for the circular-arc group is much greater for smooth wings than for wings on which a boundary-layer trip has been applied. An examination of the basic data revealed that this difference can be attributed to an unusually low value of $(dC_L/d\alpha)_0$ for the smooth sharp-trailing-edge wing (biconvex section), rather than to any unusually high values of $dC_L/d\alpha$ for the smooth blunt-trailing-edge wings. A low value of $(dC_L/d\alpha)_0$ for the 10-percent-thick biconvex airfoil might be expected in view of its sizable trailing-edge angle (approximately 22.8°), and in view of the fact that the Reynolds number of the test results presented in figure 5(f) is relatively low.

Calculations for Hypersonic Mach Numbers

The relative lift of a wedge profile compared to a symmetric double-wedge profile is shown in figure 6 as a function of Mach number for thickness ratios of 5 and 10 percent. The theoretical curves of $\Delta C_L/C_{L0}$ extend to a Mach number of 10 and were computed by shock-expansion theory. It is seen that for $t/c = 0.05$ the curves representing $\alpha = 5^\circ$ and $\alpha = 10^\circ$ are quite close together. This is a consequence of the fact that the lift curves are nearly linear over the Mach number range shown. However, it also is apparent from figure 6 that for $t/c = 0.10$ the curves representing $\alpha = 5^\circ$ and $\alpha = 10^\circ$ begin to diverge at Mach numbers above about 6, indicating that the lift curves are becoming significantly nonlinear. In view of this divergence above $M_\infty \approx 6$ for $t/c = 0.10$, it is to be expected on the basis of the hypersonic similarity rule that the curves for $t/c = 0.05$ would begin to diverge above $M_\infty \approx 12$.

At Mach numbers near 10, figure 6 shows that the relative increase in C_L at $\alpha = 10^\circ$ is appreciably greater than at $\alpha = 5^\circ$ for the 10-percent-thick airfoils. This trend is consistent with the trend that would be expected at the limit as M_∞ approaches infinity, as may be deduced from the reasoning which follows. At this limit, the surface pressure on thin airfoils is approximately proportional to the square of the local angle of inclination relative to the free-stream direction. Since the pressure on any element of surface facing downstream is zero, it follows that at $\alpha = 0^\circ$

$$\frac{dC_L}{d\alpha} \sim \int_0^c \frac{\partial P}{\partial \alpha} dx \sim \int_0^s \left(\frac{dy}{dx} \right) dx \sim y_{\max}$$

and, hence, for airfoils of equal maximum thickness, $\Delta \left(\frac{dC_L}{d\alpha} \right) / \left(\frac{dC_L}{d\alpha} \right)_0$ approaches zero as M_∞ approaches infinity, irrespective of the trailing-edge thickness or shape of the profile. On the other hand, the corresponding values of both $\Delta \left(\frac{dC_L}{d\alpha} \right) / \left(\frac{dC_L}{d\alpha} \right)_0$ and $\Delta C_L / C_{L0}$ at a finite angle are not zero. For example, the maximum value of $\Delta C_L / C_{L0}$ for a wedge airfoil compared to a double-wedge airfoil of equal thickness ratio is easily calculated from elementary calculus to be about 0.25. For thin airfoils this maximum value is independent of the thickness ratio of the two airfoils and occurs at an angle of attack approximately 4.5 times the semileading-edge angle of the wedge airfoil. Therefore, at very high supersonic Mach numbers it would be expected that $\Delta \left(\frac{dC_L}{d\alpha} \right) / \left(\frac{dC_L}{d\alpha} \right)_0$ at $\alpha = 0^\circ$ would be small, and that $\Delta C_L / C_{L0}$ would increase as α increases until a maximum (somewhat less than 0.25) is reached. As previously mentioned, such a trend is consistent with that indicated in figure 6.

In figure 7 theoretical curves of $\Delta C_L / C_{L0}$ at $\alpha = 5^\circ$ are shown as a function of Mach number for two types of airfoils, each 5 percent thick. The data points representing the present experiments at moderate supersonic Mach numbers actually represent $\Delta \left(\frac{dC_L}{d\alpha} \right) / \left(\frac{dC_L}{d\alpha} \right)_0$, but in this Mach number range the lift curves up to $\alpha = 5^\circ$ are quite linear and the two quantities are substantially equal. It is seen that the difference between the curves, one representing circular-arc airfoils and the other straight-line airfoils, is relatively small. Also, it is evident that the experimental data (except for those representing laminar flow over circular-arc sections) are in reasonable agreement with the theoretical curves.

CONCLUDING REMARKS

The effect of trailing-edge thickness on the lift-curve slope at moderate supersonic Mach numbers may be estimated with engineering accuracy by the following simple formula:

$$\frac{dC_L}{d\alpha} = \left(\frac{dC_L}{d\alpha} \right)_0 \left(1 + 1.2 \frac{h}{c} \right)$$

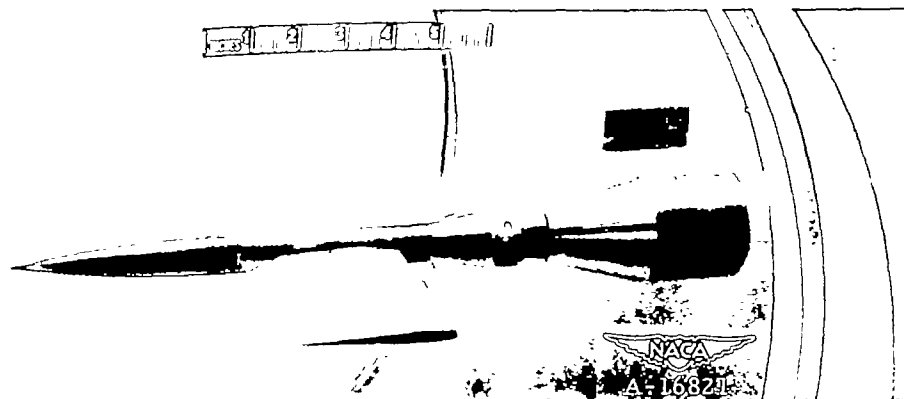
This empirical relation was obtained by plotting all data for wings with boundary-layer trips on a single graph using h/c as the abscissa. (See fig. 8.) This empirical equation, which equally well fits the mass of data for smooth wings, represents a first approximation applicable to rectangular-plan-form wings of aspect ratio greater than about 1, and at Mach numbers between about 1.5 and 3.1. The scatter of all data is such that the mean absolute deviation of $\Delta C_L/C_{L_0}$ from the empirical formula is about 0.014. If a better approximation is desired for moderate supersonic Mach numbers, the more complicated shock-expansion theory can be employed.

At hypersonic Mach numbers the lift increment of blunt-trailing-edge airfoils relative to corresponding sharp-trailing-edge airfoils is considerably larger than that given by the above empirical equation which applies only at moderate supersonic Mach numbers. Due to nonlinearities in the lift curves at high supersonic velocities, $\Delta C_L/C_{L_0}$ depends appreciably on the angle of attack and profile shape upstream of the trailing edge, as well as on the trailing-edge thickness. The theoretical calculations based on shock-expansion theory indicate, for example, that at Mach numbers between 7 and infinity, a 5-percent-thick full blunt airfoil would yield between about 15- and 25-percent-greater lift than a corresponding 5-percent-thick sharp-trailing-edge airfoil. This increase in lift is large enough so that it may be of considerable practical significance in certain cases.

Ames Aeronautical Laboratory
National Advisory Committee for Aeronautics
Moffett Field, Calif., Apr. 17, 1952

REFERENCES

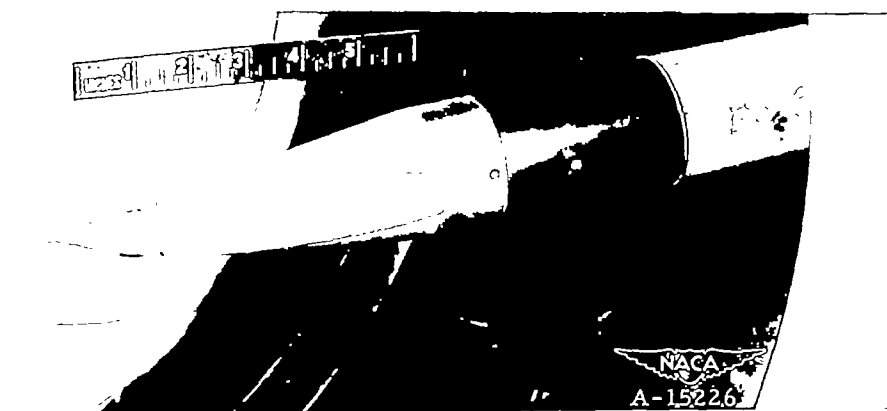
1. Busemann, A., and Walchner, O.: Aerofoil Characteristics at Supersonic Speeds. British R.T.P. Trans. 1786. (Forschung, vol. 4, no. 2, Mar./Apr. 1933, pp. 87-92).
2. Chapman, Dean R.: Reduction in Profile Drag at Supersonic Velocities by the Use of Airfoil Sections Having a Blunt Trailing Edge. NACA TN 3503, 1955. (Formerly NACA RM A9H11.)
3. Chapman, Dean R., Wimbrow, William R., and Kester, Robert H.: Experimental Investigation of Base Pressure on Blunt-Trailing-Edge Wings at Supersonic Velocities. NACA TN 2611, 1952.



(a) Wing of thickness group mounted on body support.

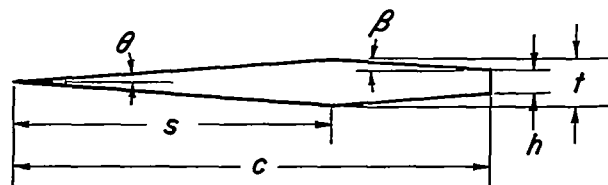


(b) Wing of thickness group mounted on sting support.



(c) Wing of circular-arc group mounted on asymmetric sting support.

Figure 1.— Photographs of typical model installations.



$\beta = \theta$ for all airfoils of this group

Profile		t/c	h/t	h/c	s/c	β
	*	0.10	0	0	0.500	5.71°
		0.10	0.25	0.025	0.572	5.00°
	*	0.10	0.50	0.050	0.667	4.28°
		0.10	0.75	0.075	0.800	3.58°
	*	0.10	1.00	0.100	1.000	-2.87°
		0.075	0	0	0.500	4.29°
		0.075	0.25	0.0188	0.572	3.75°
		0.075	0.50	0.0375	0.667	3.22°
		0.075	0.75	0.0562	0.800	2.68°
		0.075	1.00	0.075	1.000	-2.15°
	*	0.05	0	0	0.500	2.86°
		0.05	0.25	0.0125	0.572	2.50°
	*	0.05	0.50	0.025	0.667	2.15°
		0.05	0.75	0.0375	0.800	1.78°
	*	0.05	1.00	0.050	1.000	-1.43°

(a) Airfoils of the thickness group; $A = 3$; asterisk (*) indicates that $A = 2$ and 1 were also tested.



Figure 2.—Profiles and geometric characteristics of airfoils investigated.

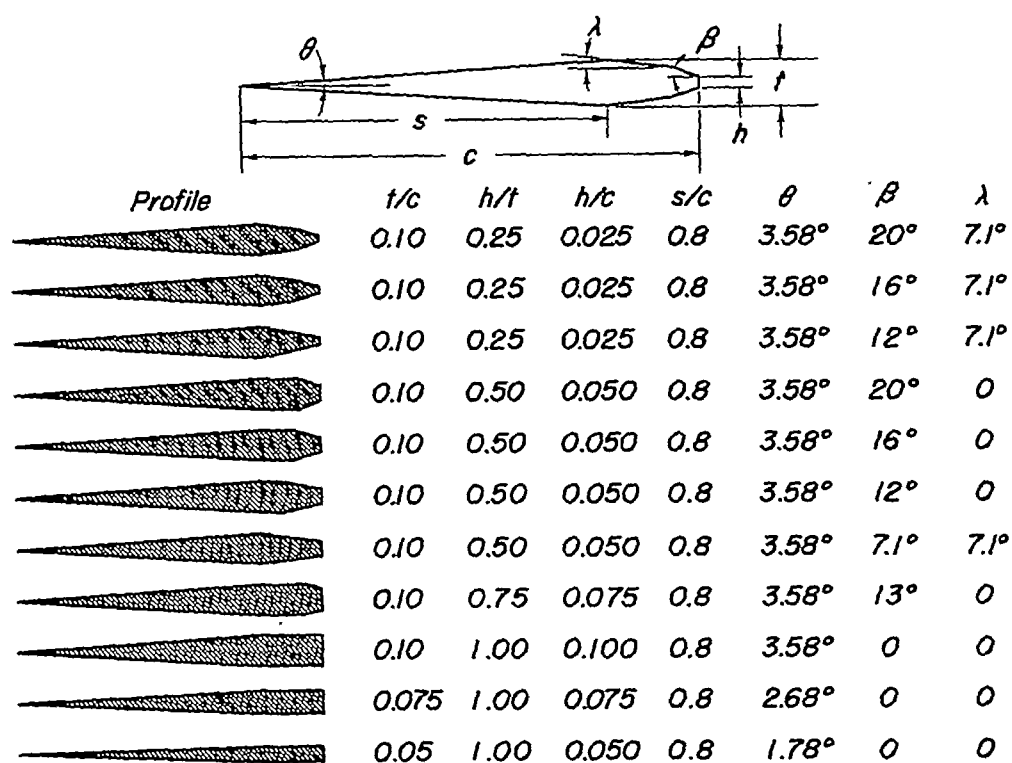
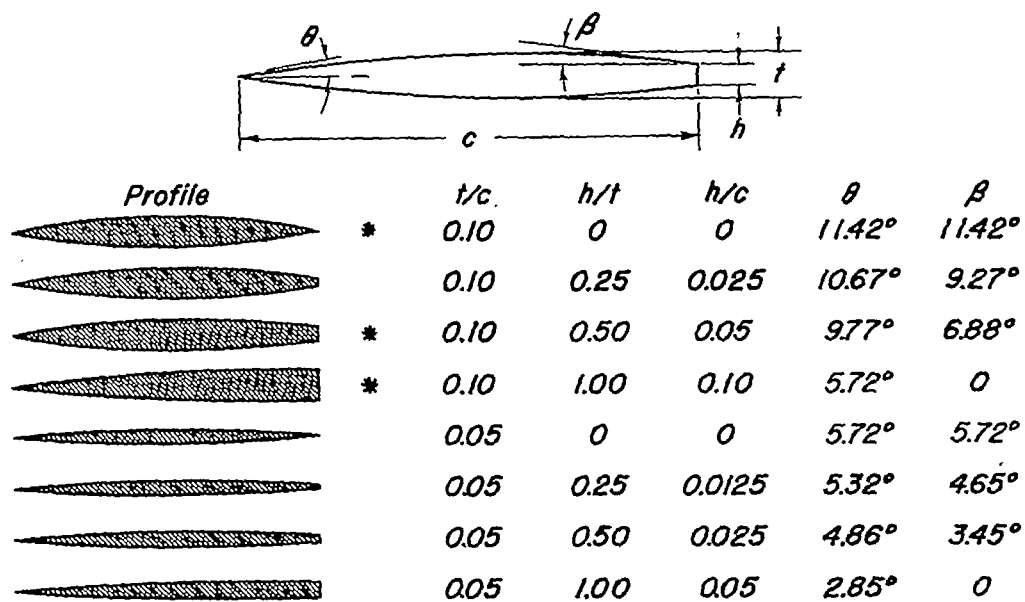
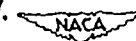
(b) Airfoils of the boattail group; $A = 3$.(c) Airfoils of the circular-arc group; $A = 4$; asterisk (*) indicates that $A = 3.5, 3, 2.5, 2, 1.5$, and 1 were also tested.

Figure 2.- Concluded.



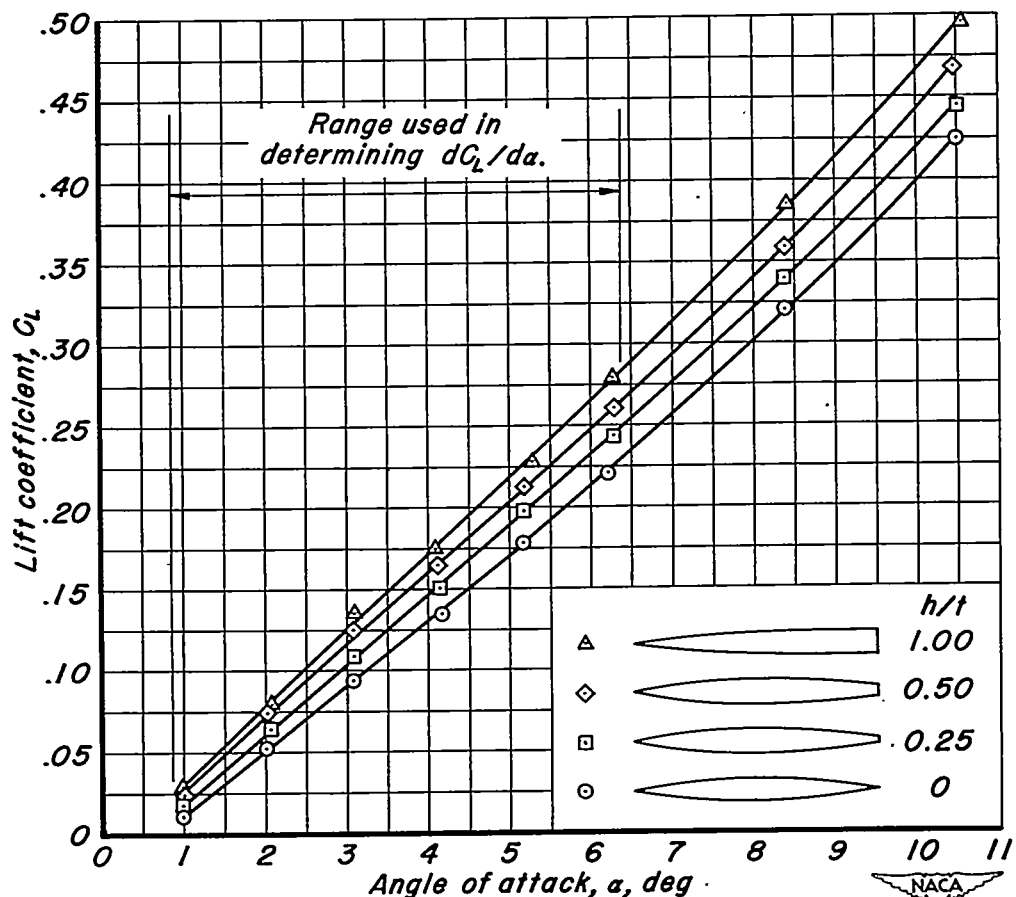


Figure 3.- Typical lift curves for smooth wings of the circular-arc group; $t/c=0.10$, $A=4$, $M_\infty=2.0$, $Re=0.55 \times 10^6$.

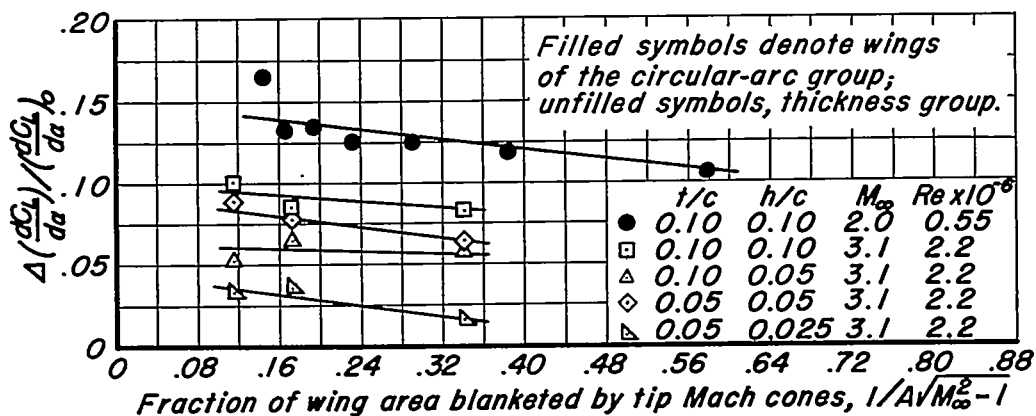


Figure 4.- Fractional increase in lift-curve slope for smooth wings of various aspect ratio.

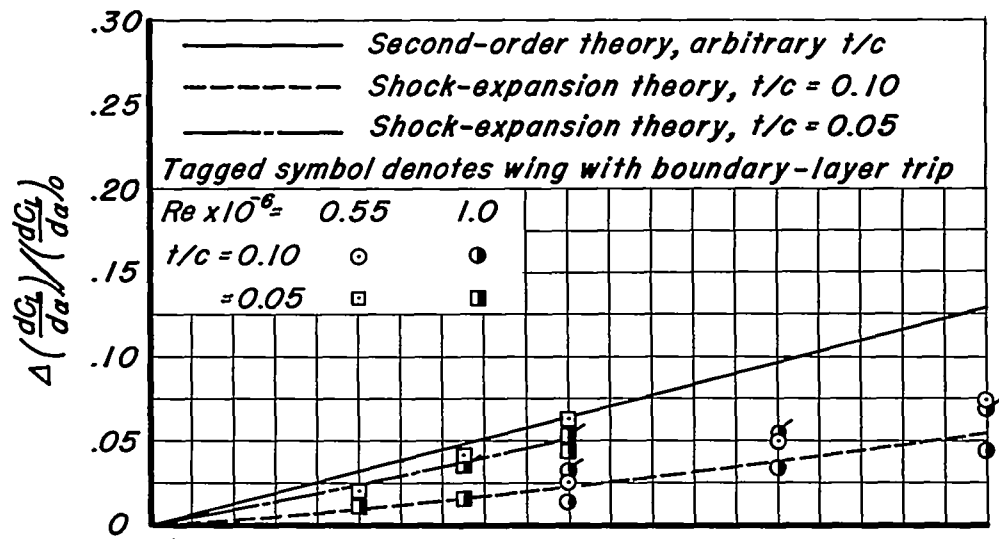
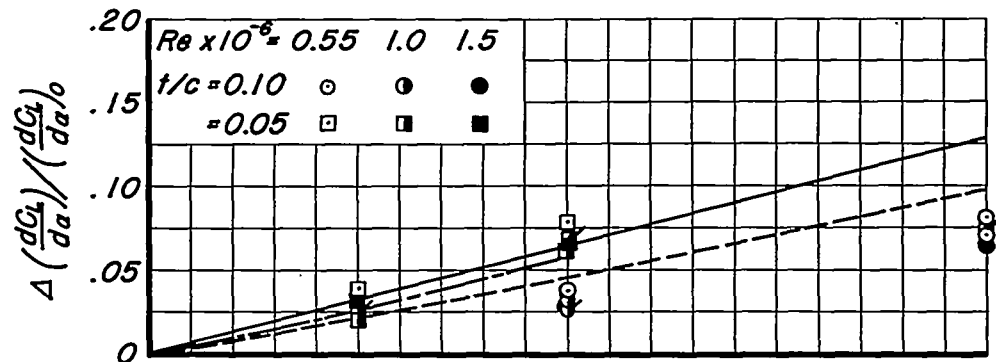
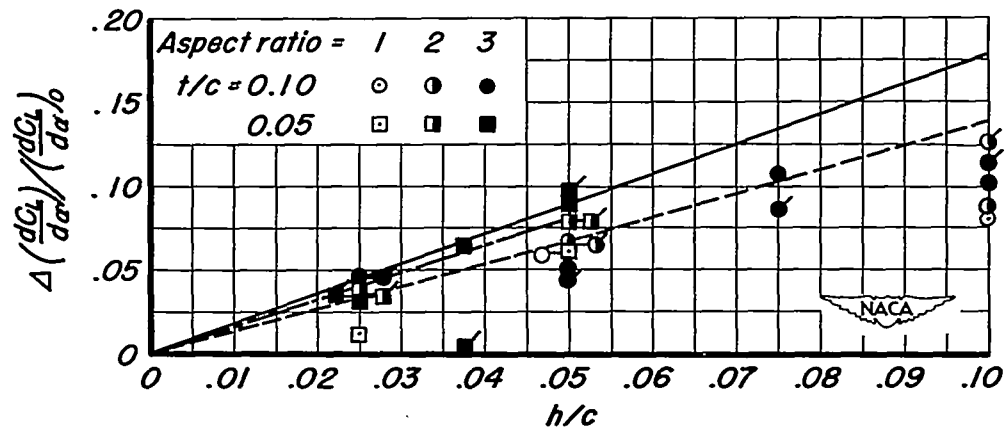
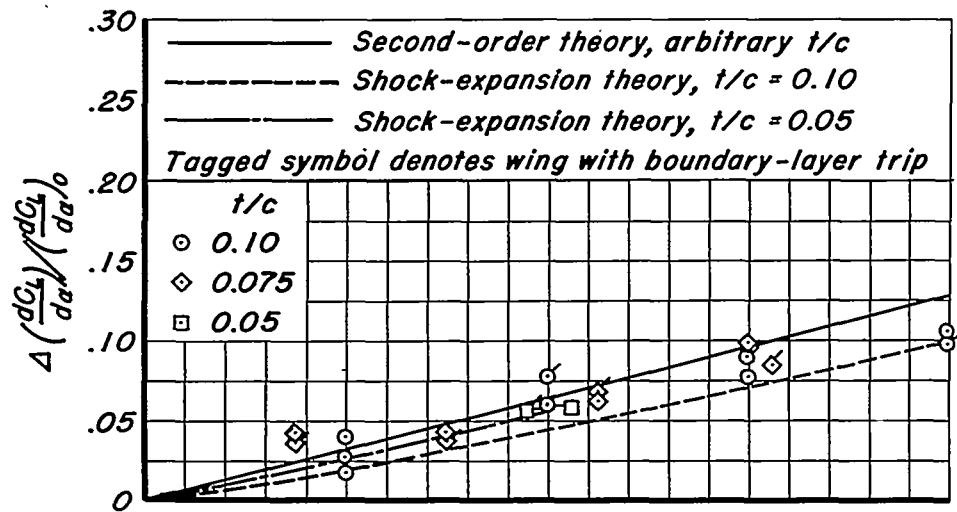
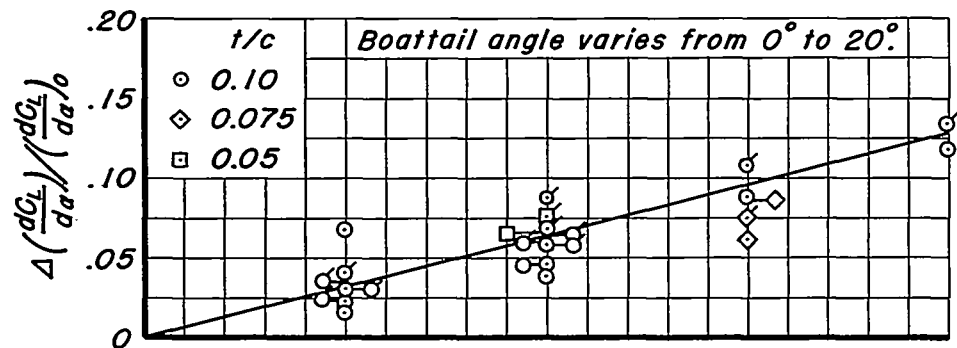
(a) Thickness group, body support, $M_\infty = 1.5$, $A = 3$.(b) Thickness group, body support, $M_\infty = 1.9$, $A = 3$.(c) Thickness group, body support, $M_\infty = 3.1$, $Re = 2.2 \times 10^6$.

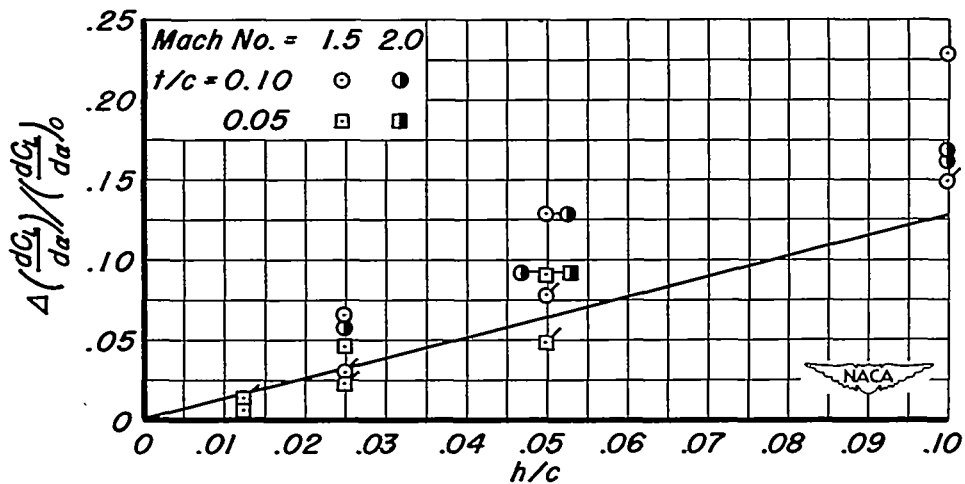
Figure 5.—Effect of trailing-edge thickness on fractional increase in lift-curve slope.



(d) Thickness group, sting support, $M_\infty 2.0$, $Re = 1.0 \times 10^6$, $A = 3$.



(e) Boattail group, sting support, $M_\infty 2.0$, $Re = 1.0 \times 10^6$, $A = 3$.



(f) Circular-arc group, sting support, $Re = 0.55 \times 10^6$, $A = 4$.

Figure 5.— Concluded.

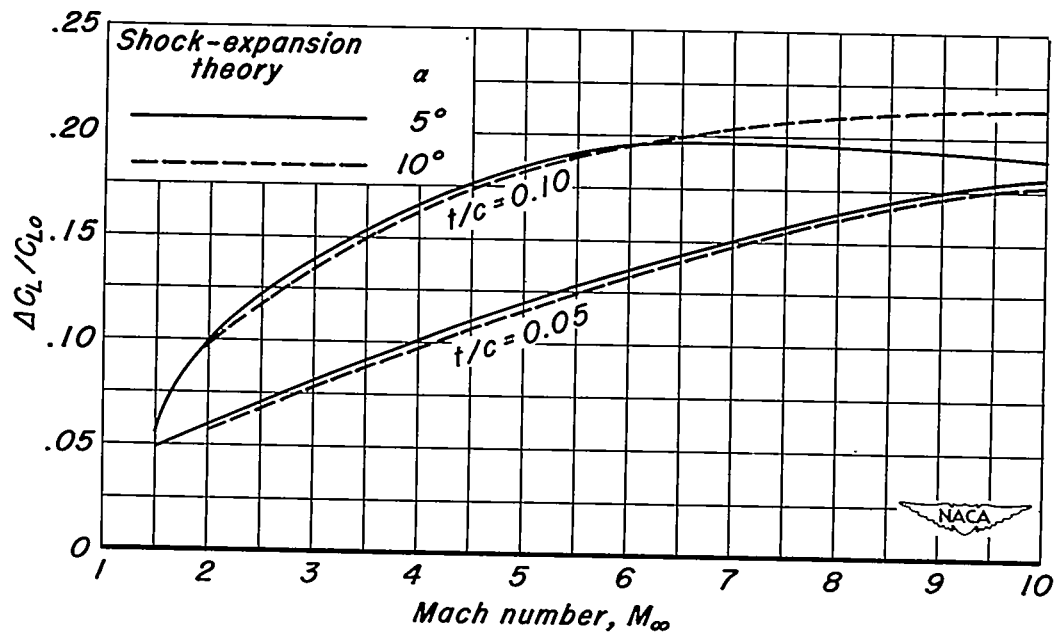


Figure 6.—Lift increment of wedge airfoil relative to double-wedge airfoil.

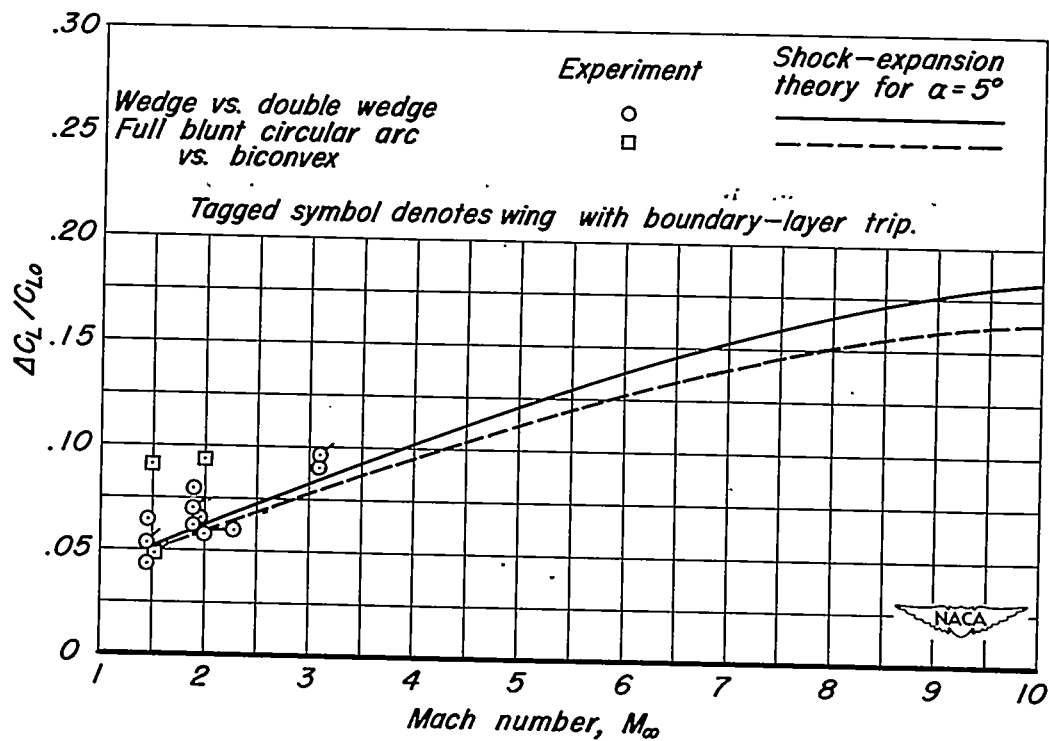


Figure 7.—Lift increment of 5-percent-thick full-blunt airfoils relative to corresponding sharp-trailing-edge airfoil.

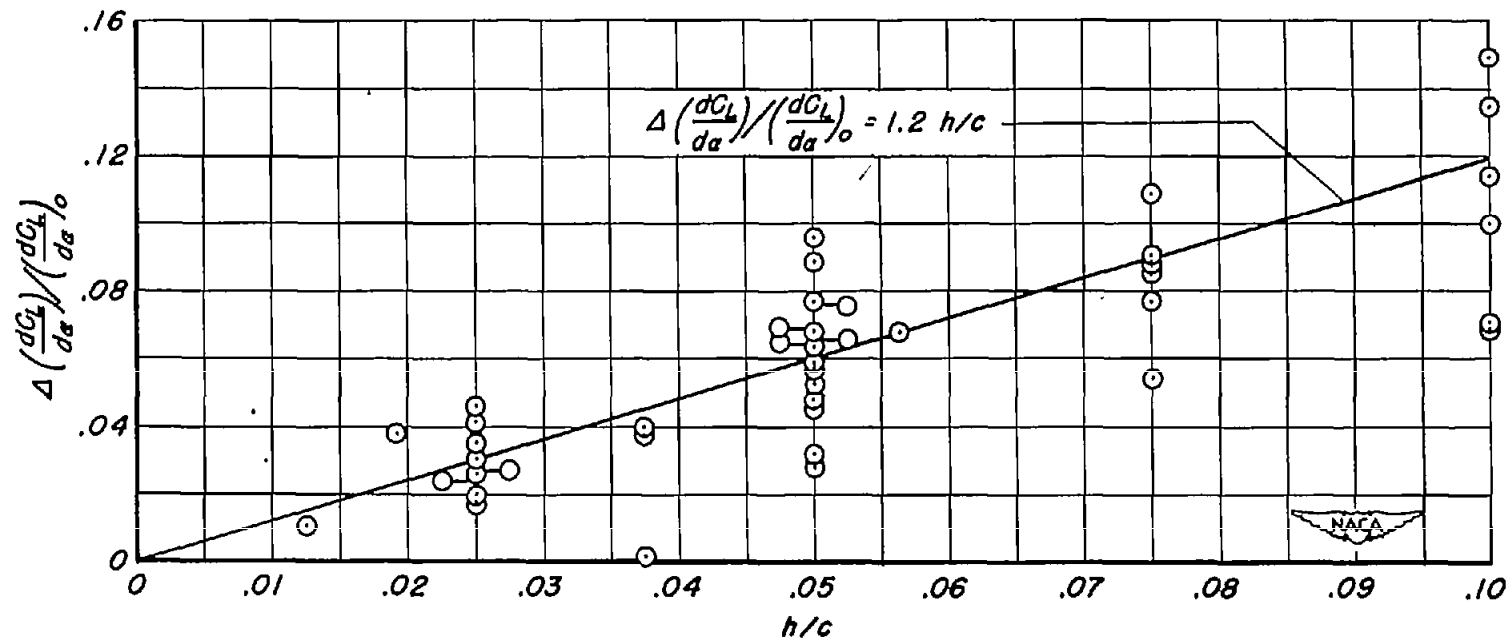


Figure 8.- Compilation of data for turbulent flow (tagged symbols in figure 5) over wings of thickness, boattail, and circular-arc groups for all values of thickness ratio, Mach number, and Reynolds number investigated; $A = 3$ and 4.